SANDIA REPORT

SAND2016-9886
Unlimited Release
Printed September 2016

Reverberation Chamber Characterization

Robert A. Salazar, Megan E. Daily, Matt Halligan, Joseph M. Rudys, Michael L. Horry

Prepared by
Sandia National Laboratories
Albuquerque, New Mexico 87185 and Livermore, California 94550

Sandia National Laboratories is a multi-mission laboratory managed and operated by Sandia Corporation, a wholly owned subsidiary of Lockheed Martin Corporation, for the U.S. Department of Energy's National Nuclear Security Administration under contract DE-AC04-94AL85000.

Issued by Sandia National Laboratories, operated for the United States Department of Energy by Sandia Corporation.

Available to DOE and DOE contractors from
U.S. Department of Energy
Office of Scientific and Technical Information
P.O. Box 62
Oak Ridge, TN 37831

Telephone: (865) 576-8401
Facsimile: (865) 576-5728
E-Mail: reports@osti.gov
Online ordering: http://www.osti.gov/scitech

Available to the public from
U.S. Department of Commerce
National Technical Information Service
5301 Shawnee Rd
Alexandria, VA 22312

Telephone: (800) 553-6847
Facsimile: (703) 605-6900
E-Mail: orders@ntis.gov
Online order: http://www.ntis.gov/search

SAND2016-9886
Unlimited Release
Printed September 2016

Reverberation Chamber Characterization

Robert A. Salazar, Megan E. Daily, Joseph M. Rudys, Michael L. Horry
Electrical Sciences & Experiments, Dept. 1353
Sandia National Laboratories
P.O. Box 5800
Albuquerque, New Mexico 87185-MS1152

Abstract

In this study, we characterized and quantified the behavior of Sandia National Laboratories' electromagnetic reverberation chamber owned by department 1353. The primary purpose of the chamber is to measure the response of a test object to electromagnetic stimuli. The primary chamber application is qualification of nuclear weapons systems and components for the nuclear weapon qualification programs. National Nuclear Security Administration (NNSA) requires a comprehensive understanding of any measurement used to qualify a nuclear weapon. Understanding includes the accuracy of every measurement used to qualify the weapon. Knowing the uncertainty of any measurement gives the information needed to estimate boundaries and tolerances of the measurement. By proper application of these measurement tolerances, weapon qualification programs can comply with uncertainty requirements. This document reports our findings.

Weapons Systems Engineering Assessment Technology (WSEAT) commissioned this effort to provide support to Nuclear Weapons qualification in accordance with Realize Product Sub System (RPSS). Motivation for this effort stems from four qualification programs: B61 LEP, W88 ALT370, W80-4 LEP, and the Mk21 fuze program.

ACKNOWLEDGMENTS

The authors would like to acknowledge support received in executing these measurements and performing a review of this document. Reviewers for formatting and technical content include: Clare Amann, Matt Halligan, Mark Jursich, Steve Glover, Larry Warne, Mike Dinallo, and Lorena Basilio.

CONTENTS

1. Introduction....9
2. Description of Reverberation Chamber....11
3. Test Objectives....13
4. Test Setup....15
5. Test Requirements....17
   5.1 Lowest Usable Frequency (LUF)....17
   5.2 Chamber quality (Q) Factor....17
   5.3 Sampling requirements....17
6. Test Methodology....19
   6.1 Data collection....19
   6.2 Probe placement....19
   6.3 Data Processing....20
7. Results....25
8. References....41
Distribution....42

FIGURES

Figure 1 Reverberation Chamber Diagram....11
Figure 2: Instrumentation Setup....16
Figure 3: Reverberation Chamber Probe Placement....20
Figure 4: Monopole modeled parameters for E-field conversion data....23
Figure 5: Max and Mean Electric Field Measured Using Electric Field Probes....25
Figure 6: Comparison of Electric Field Measurements with Theoretical Distribution....26
Figure 7: Mean Normal Standard Deviation for different rotation speeds....27
Figure 8: Estimated number of identical and independent samples....28
Figure 9: Max and Mean Received Power from Monopole Sensors on Walls....29
Figure 10: Electric Field Calculated from Monopole Measurements....30
Figure 11: Cumulative Distribution Function for Power Readings....31
Figure 12: Standard Deviation of 8 Corner Points of Working Volume....32
Figure 13: Lower Volume....33
Figure 14: Upper Volume....34
Figure 15: Total volume....35
Figure 16: Reduced data collection....36
Figure 17: Comparison of Monopole and Electric Field Probe Measurements....37
Figure 18 Comparison of ETS probe and monopoles E-field strength....38

NOMENCLATURE

dB	decibel
DOE	Department of Energy
DUT	Device under test
EUT	Equipment under test
E-field	Electric field
EM	Electromagnetic
EMES	Electromagnetic Environment Simulator
EMP	Electromagnetic Pulse
EMR	Electromagnetic Radiation
GTEM	Gigahertz Transverse Electromagnetic
NW	Nuclear Weapons
RF	Radio Frequency
RPSS	Realize Product Sub System
SNL	Sandia National Laboratories
TDR	Time Domain Reflectometer
TEM	Transverse Electromagnetic
V/m	Volts per meter
W	Watt

1. INTRODUCTION

In this document, we report results from a sequence of measurements conducted in the reverberation chamber between July 2015 and September 2015. Some additional results obtained September 2016 augment this report. The purpose of these measurements was to obtain information about the behavior and performance of the reverberation chamber with regard to electromagnetic properties (Q, peak fields, etc.). This information provides the capability to characterize the uncertainty of measurements made in the chamber. Department 1353 (Electrical Sciences) uses the chamber to measure the behavior of different components and systems susceptible to electromagnetic interference.

Typically, measurements fall into two classes 'transfer functions' and 'system susceptibility'. These two classes of measurements further divide into categories. For transfer functions, the categories include but are not limited to:

1. Shielding effectiveness
2. Effective height
3. Induced current

In each of the transfer functions, a transducer measures a parameter of interest within a test object. E-field sensors located on the walls of the reverberation chamber measure the electric field in the reverberation chamber. The ratio of the parameter of interest to measured electric field within the chamber yields a transfer function. Units of transfer functions depend on the measured parameters. Application of the transfer function to a linear system allows one to compute an equivalent parameter value for an arbitrary E-field value. For example, an induced current will have units of Amperes/(Volt/meter). Given a transfer function value of 11 (mA/(V/m)) for an electronic component, one can predict a hypothetical E-field of 1000 V/m yielding 11 A in a test object. This result may then translate to an acceptance or rejection of the object to a specific environment. In this example, a transfer function provides the information needed for an analysis to determine if an electronic component is acceptable for use in a system that may experience a specific electromagnetic environment.

A second class of measurement, susceptibility, is sometimes necessary. System or component data allowing the prediction of an undesired effect due to an induced current or other parameter may not exist. Due to system nonlinear behavior and interactions in an electronic system, a demonstration of an object's response to an E-field at the correct amplitude may be necessary. This second class of measurements involves a direct measure of electromagnetic influence on a test object. In the example described above, if there is uncertainty about the transfer function value or the effect occurring at 11 A is not certain, a full strength E-field upset test may be necessary to ensure an accurate measure of the E-field influence on a test object. A more direct test would set the E-field in the reverberation chamber to a known value and detect if the test

object reacts to the insult. Sensors in the test object reports the response of the test object to the E-field. If the test object is functional during the test, monitors can detect any test object observables for disruption or disturbance.

2. DESCRIPTION OF REVERBERATION CHAMBER

In this study, we characterized and quantified the behavior of Sandia National Laboratories electromagnetic reverberation chamber. The primary use of the chamber is to measure the response of a test object to an electromagnetic environment. The chamber is 11 m by 7 m by 4 m of welded aluminum. The aluminum walls are low loss; hence, low injected power creates large electric fields. The chamber sources are seven solid-state or traveling-wave tube (TWT) amplifiers capable of delivering 1 kW between 220 MHz and 18 GHz and 40 W between 18 GHz and 40 GHz. The fields produced inside the chamber are pseudo-randomly directional and non-planar in nature entering the chamber via antennas. A rotating tuner creates a chaotic field behavior in the reverberation chamber. Monopole antennas mounted on the chamber walls are transducers converting the chamber E-field to a voltage. Power meters measure the antenna voltages and convert the voltages to equivalent power readings. With well-known monopole characteristics, the LabVIEW™ code converts the detected powers to the E-fields in the chamber working volume. One significant assumption is the E-field at any point on the wall is equal to the E-field at any other location on the wall. Further, the E-field measured at the wall is 3 dB greater than the E-field at any location in the chamber. Therefore, the LabVIEW™ code corrects the reading and records the chamber working volume E-field.

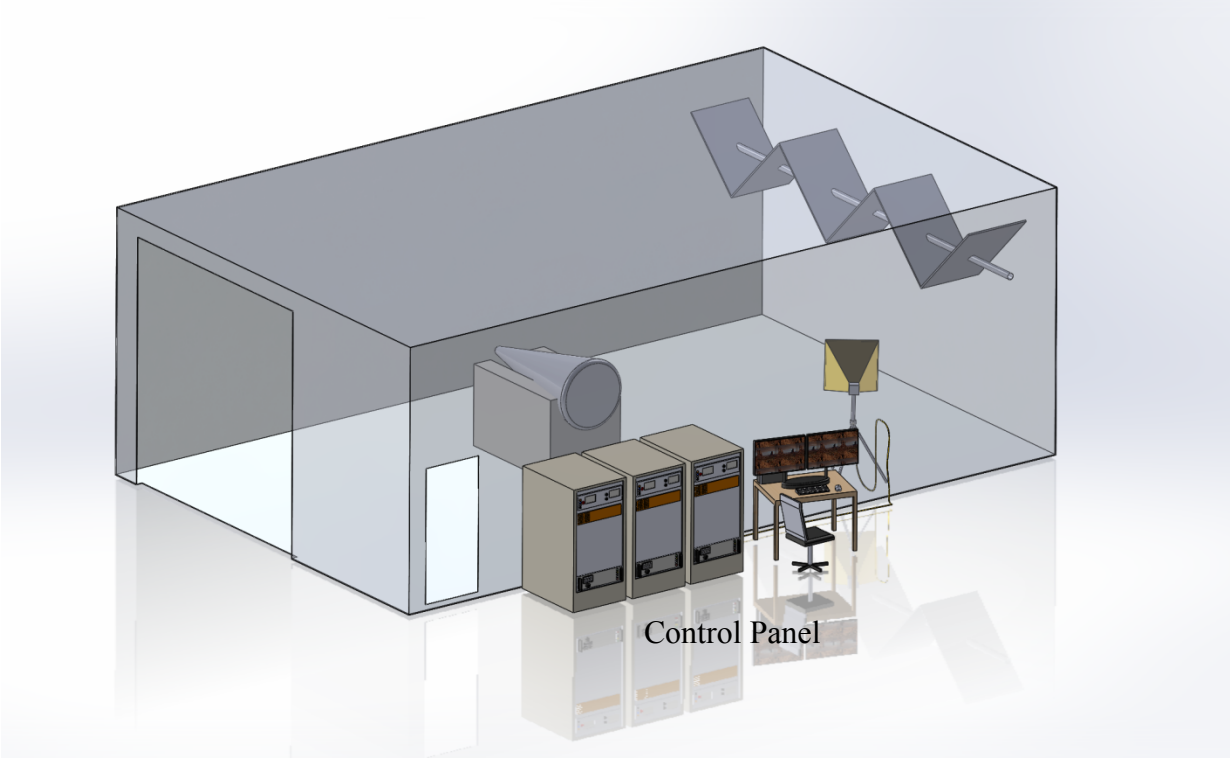

Figure 1 Reverberation Chamber Diagram

A reverberation chamber produces an E-field with statistically uniform amplitude for any orientation and polarization in any location in the chamber. This is a very powerful situation allowing the testing of an object without regard to its placement in the chamber. The IEC standard[1] states that the test object shall not exceed 8 % of the chamber volume as a requirement. The chamber is 308 m^3; therefore, the test object can occupy up to 24.6 m^3. There is no limit to the number of objects in the chamber provided the aggregate object volume does not exceed 8 % of the chamber volume.

Four sets of monopoles measure the E-field on three walls and the ceiling. Power meters measure power at each monopole. The data acquisition software computes the statistics of the different probes providing a measure of the E-field at the walls. The reverberation chamber currently only executes mode stirring. Hence, the tuner is in constant motion over the time of a single measurement. Chamber software controls the rate of the tuner rotation with a minimum rotation time of 5 seconds. During one rotation, the acquisition software sets the sample rate of the power meters to acquire 1000 measurements for one revolution. The acquisition software computes the statistics for 1000 measurements for each monopole. One can then compare the results between the four monopoles and determine the uniformity of the E-field at the four locations.

The data acquisition software sets the injected power from the power amplifies into the chamber by using measured injected power via a directional coupler. Once the power is set, the power meters make the 1000 measurements over one tuner rotation. The control software repeats this process for the frequencies prescribed by the chamber operator. For the full frequency capability, (200 MHz to 40 GHz) seven different amplifiers and instrumentation sets deliver and measure the injected and reflected power of the amplifiers for testing at each frequency step. The same data acquisition software controls the E-field measurement at the chamber wall and any transducer place inside or on the test object.

[1] **A.5.5 Loading effects**

3. TEST OBJECTIVES

The objective of this effort was to quantify the uncertainty of the E-field in the reverberation chamber over its working volume. To achieve this objective we followed the instruction of IEC 61000-4-12. The IEC standard provides methodology and requirements for characterizing and quantifying the performance of reverberation chambers. Although the international community recognizes this IEC standard, RPSS does not require compliance. We simply used this as a best practice reference to evaluate the performance the reverberation chamber.

4. TEST SETUP

Following guidance provided by IEC 61000-4-21, we placed probes inside the working volume of the chamber and executed the chamber data acquisition software over the full range of the test. Three ETS HI-6153 probes, mounted on a single dielectric stand, measured all the E-field values in the working volume of the chamber. Each probe uses a fiber optical interface between the probes and the instrument controls.

Figure 2 shows the instrumentation setup for the reverberation chamber. Staff personnel keep the instrument calibrations up to date as required by RPSS.

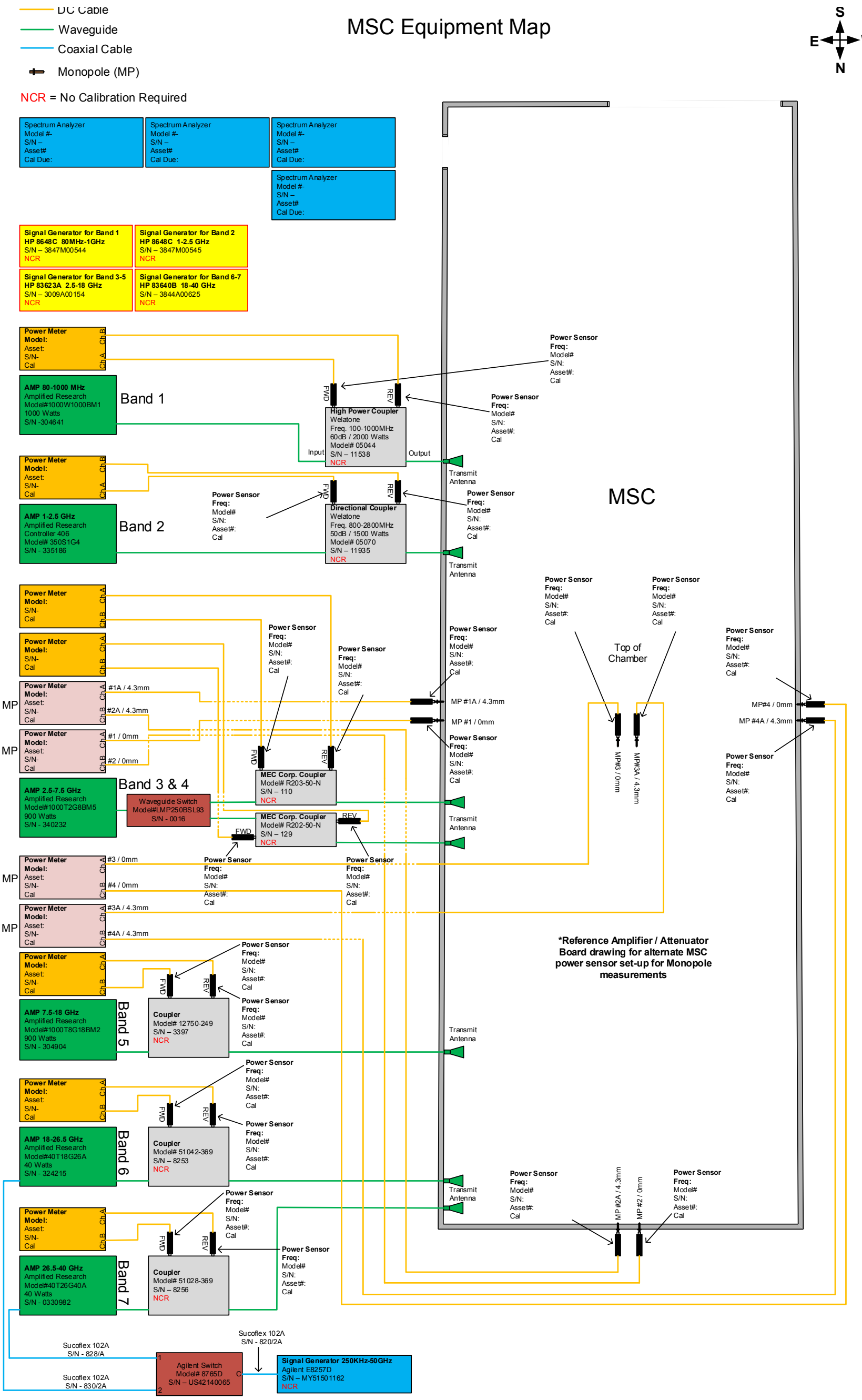

Figure 2: Instrumentation Setup

5. TEST REQUIREMENTS

IEC 61000-4-21 is an industry standard that defines a methodology to quantify the uniformity of a reverberation chamber. We used this standard as a general guide to execute this effort.

5.1 Lowest Usable Frequency (LUF)

The lowest usable frequency described in the standard is the frequency where the specified field uniformity meets the standard requirements. The standard defines the working volume by the eight corner locations of the volume. There is no requirement for a specific lowest frequency.

5.2 Chamber quality (Q) Factor

The ability of the chamber to store energy relative to the rate of dissipation is a measure of the chamber Q. Factors influencing the value of Q are frequency, chamber volume, wall material, object material, and the test object size. Any apertures, including antennas, reduce the chamber Q. There is no requirement for Q. However, Q is an indicator of the achievable E-field for a given drive power.

5.3 Sampling requirements

Table 1 of [1] sets the required number of independent samples and frequency measurement. All measurements for this effort exceed the sampling requirement.

Table 1. Sampling requires from table B1 of [1]

Frequency range	Minimum number of samples required for validation and test	Number of frequencies required for validation
f_s to 3 f_s	12	20
3 f_s to 6 f_s	12	15
6 f_s to 10 f_s	12	10
Above 10 f_s	12	20/decade
f_s is the lowest test frequency		

6. TEST METHODOLOGY

6.1 Data collection

To understand the data collected for the effort, one needs to understand how the instrumentation software operates the chamber. A LabVIEW™ program operates all the equipment, collects, and processes all the data. At the beginning of every test series, the reverberation chamber operator starts the LabVIEW™ program. The operator verifies that all the instruments settings are correct and sets the parameters of the test. The parameters include power, frequency range, increment size, and many other parameters. The frequency range and the increment size establish the number of data points collected in an entire run. Once the operator enters all the parameters, the operator then executes the data collection code.

The main LabVIEW™ program runs the reverberation chamber exclusively in a 'stirred mode'. The operator sets a fixed tuner speed rotation. All instruments gather 1000 samples over one rotation period. Hence, for the minimum speed of 5 seconds per revolution the instruments sample every 5 milliseconds. The angular change between samples of the tuner is ~0.36 degrees.

While the tuner is rotating, the program turns on the amplifier and sets the RF source frequency and power to deliver a fixed power level into the chamber at a frequency set by the program. After the power and frequency are set, four power meters collect data from four monopoles. In almost all tests, spectrum analyzers measure RF energy from transducers in or on a test object. The LabVIEW™ program controls the spectrum analyzers selected by the operator for a test. The operator sets the parameters of the spectrum analyzers. The spectrum analyzers collect information from transducers located on or in the test object. For this chamber characterization test, ETS probes detected E-field at the location defined in the field map. The ETS probes collected 1000 samples for each tuner revolution.

6.2 Probe placement

IEC 61000-4-21 provides guidance regarding probe placement. Eight probes create a box that bound a volume used to characterize the field uniformity of the volume in the reverberation chamber. In this effort, we use three boxes to show statistical variation over the chamber volume. Figure 3 shows probe placement (short cylinders at each corner) for the three volumes. The probe locations define the volume locations. Figure 3 shows two volumes. The two volumes combine to create a third larger volume. Later in the report, Volume 1 is referred to as the top volume, Volume 2 is the bottom volume, and the combination of the two volumes is the full volume.

Figure 3 shows the stack of three probes that collected data at each probe location. One probe was at the center height of the chamber. One probe was 1 meter above the center probe and one probe was 1 meter below the center probe. In this paper, we present data from 12 unique locations – four probe stand locations and three probe heights. The two probe stand locations

nearest the large door are 1m from each wall and the probe stands nearest the stirrer are 5.6m away from the first probe stands to allow sufficient clearance for the stirrer and antennas as well as 1m from the walls. The probes measuring the electric fields are commercially available ETS tri-axial electric field probes model number HI-6153.

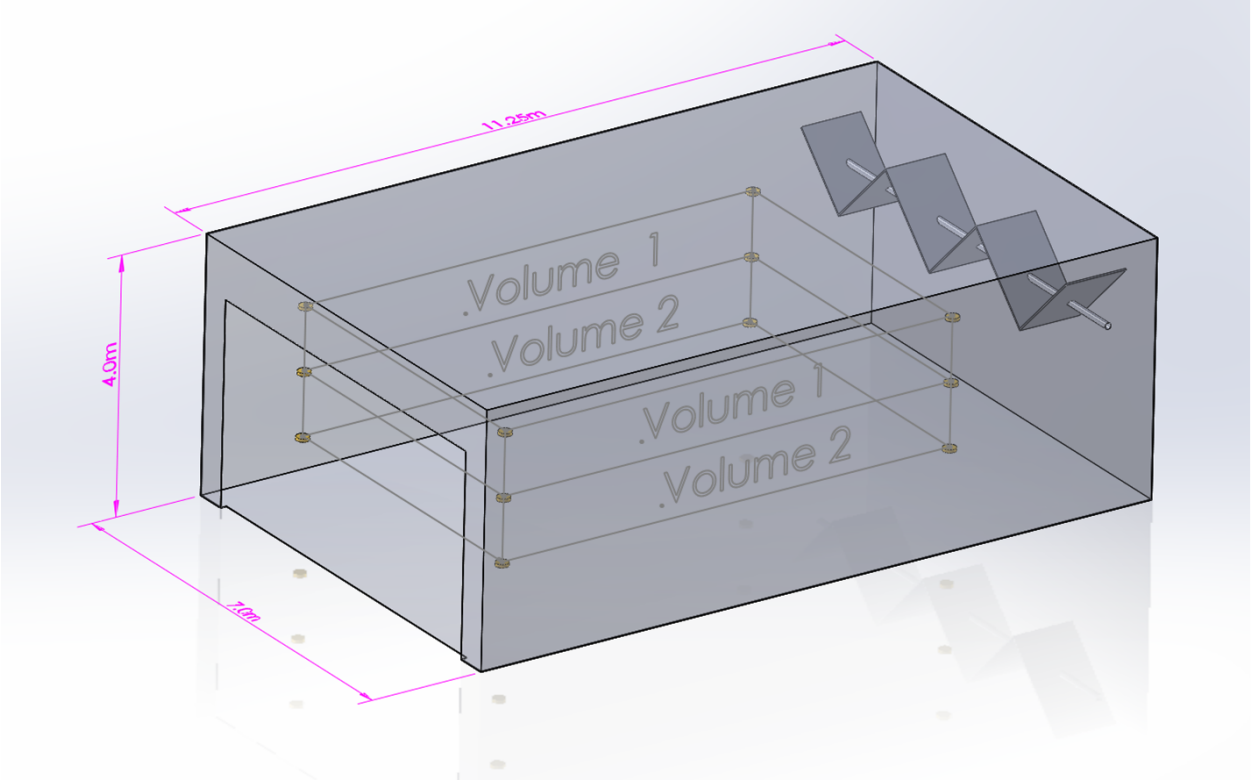

Figure 3: Reverberation Chamber Probe Placement

6.3 Data Processing

IEC 61000-4-21 delineates a process for evaluating the uniformity of the E-field in a reverberation chamber. The standard assumes the reverberation chamber uses 'mode tuning'; however, 'mode stirring' is acceptable with proper operational restrictions.

As mentioned earlier, during one revolution of the tuner, instrumentation produces 1000 data points for each location constructing the statistics presented in this paper. Each location has a probe that captures the three dimensional E-field in the chamber. The following description focuses on a single location.

These results use calibration corrected data. We computed the statistics for each element of each probe. The element labels are 'X', 'Y', 'Z'. The labels do not correspond to any particular direction, but they are orthogonal to each other.

The theoretical distribution of the E-field at very high frequencies is a chi distribution with two degrees of freedom. [2-3]

$$CDF\left\{\chi\left(\frac{E}{\mu}\right)\right\} = 1 - e^{\left(-\frac{\pi}{4}\left(\frac{E}{\mu}\right)^2\right)}$$

$$where, \frac{E}{\mu} is\ the\ E\text{□} - field\ normalized\ to\ the\ E - field\ mean$$

Equation 1. Chi distribution

Analysis in this paper uses the Kolmogorov-Smirnov Goodness-of-Fit Test to evaluate how well measured results fit theory. [4]

$$D = \max_{1 \le i \le N}\left(F(Y_i) - \frac{i-1}{N}, \frac{i}{N} - F(Y_i)\right)$$

where F is the theoretical cumulative distribution of the distribution being tested

Equation 2. Kolmogorov-Smirnov Goodness-of-Fit

Another metric of performance is an estimate of the number of identical and independent samples. The standard employs the use of autocorrelation to determine when a datum point is independent of the previous datum point.

$$r = \frac{\frac{1}{n-1}\sum_i^n (x_i - \mu_x)(y_i - \mu_y)}{\frac{\sum_i^n (x_i - \mu_x)^2}{n-1}\frac{\sum_i^n (y_i - \mu_y)^2}{n-1}}$$

Equation 3. Sample set autocorrelation [1]

Since the mode density increases with increasing RF frequency, the number of independent samples also increases with RF frequency.

Another metric of chamber performance is the mean normalized standard deviation. Assuming a chi distribution with 2 degrees of freedom the expected statistical values are:

$$\sigma = \left(2 - \frac{\pi}{2}\right)^{\frac{1}{2}}$$

$$\mu = \left(\frac{\pi}{2}\right)^{\frac{1}{2}}$$

$$\frac{\sigma}{\mu} = \left(\frac{\pi}{2}\right)^{\frac{1}{2}} \sim 0.5227$$

Four monopoles serve as transducers integrated into the reverberation chamber walls to measure E-field. Power meters measure the power from each monopole and the control software collects, processes, and records the information into a data file. For improved sensitivity, 4.3 mm length monopoles collect data below 18 GHz. Above 18 GHz the 4.3 monopoles resonate, so the control instrumentation collects data from 0.0 mm length monopoles above 18 GHz to the full capability of the chamber of 40 GHz. The power meters have a noise floor of -60 dBm and 1 dB compression value of +10 dBm. Power above +20 dBm may damage the power meters. The results section of this report will show a dramatic drop of detected power at 18 GHz, which is a consequence of the transition from the 4.3 mm monopoles to the 0.0 mm monopoles. The control software applies the correct probe calibration and records the corrected E-field to the data file.

To evaluate the monopole power measurement, we compute the chi-squared cumulative distribution function and compare the monopole power to the expected results. [3], [5]

Equation 4 shows the cumulative distribution function.

$$CDF\left\{{\chi_2}^2\left(\frac{P}{\mu}\right)\right\} = 1 - e^{-\left(\frac{P}{\mu}\right)}$$

Equation 4. Chi-square distribution with two degrees of freedom

The power meter results convert to E-field using

Equation 5. Information needed to compute the E-field includes knowledge of the monopoles.

Equation 5 uses the monopole impedance and effective height to compute the E-field.

$$E_n = \sqrt{\frac{P_L Z_a + Z_L}{Z_L \quad h_{eff}}}$$

Z_a is the monopole impedance
Z_L is the meter impedance
h_{eff} is the probe effective height

Equation 5. Power reading converted to E-field measurement

Figure 4 shows the conversion information for the monopoles. The control software implements Equation 5 and makes any added corrections including cable losses.

IEC 61000-4-21 provides a procedure to compute and evaluate the uniformity of the chamber. The mean and the standard deviation of the eight points provide the information needed to evaluate field uniformity of the volume occupied within the eight points. The ratio of the maximum field strength to forward power—Equation 6—is the normalized maximum E-field. The input power is in units of watts and the E-field comes from each of the three axes.

$$\vec{E}_{x,y,z} = \frac{E_{Max\ x,y,z}}{\sqrt{P_{Input}}} \left(\frac{\left(\frac{V}{m}\right)}{\sqrt{watt}} \right)$$

Equation 6. Normalized Maximum E-field.

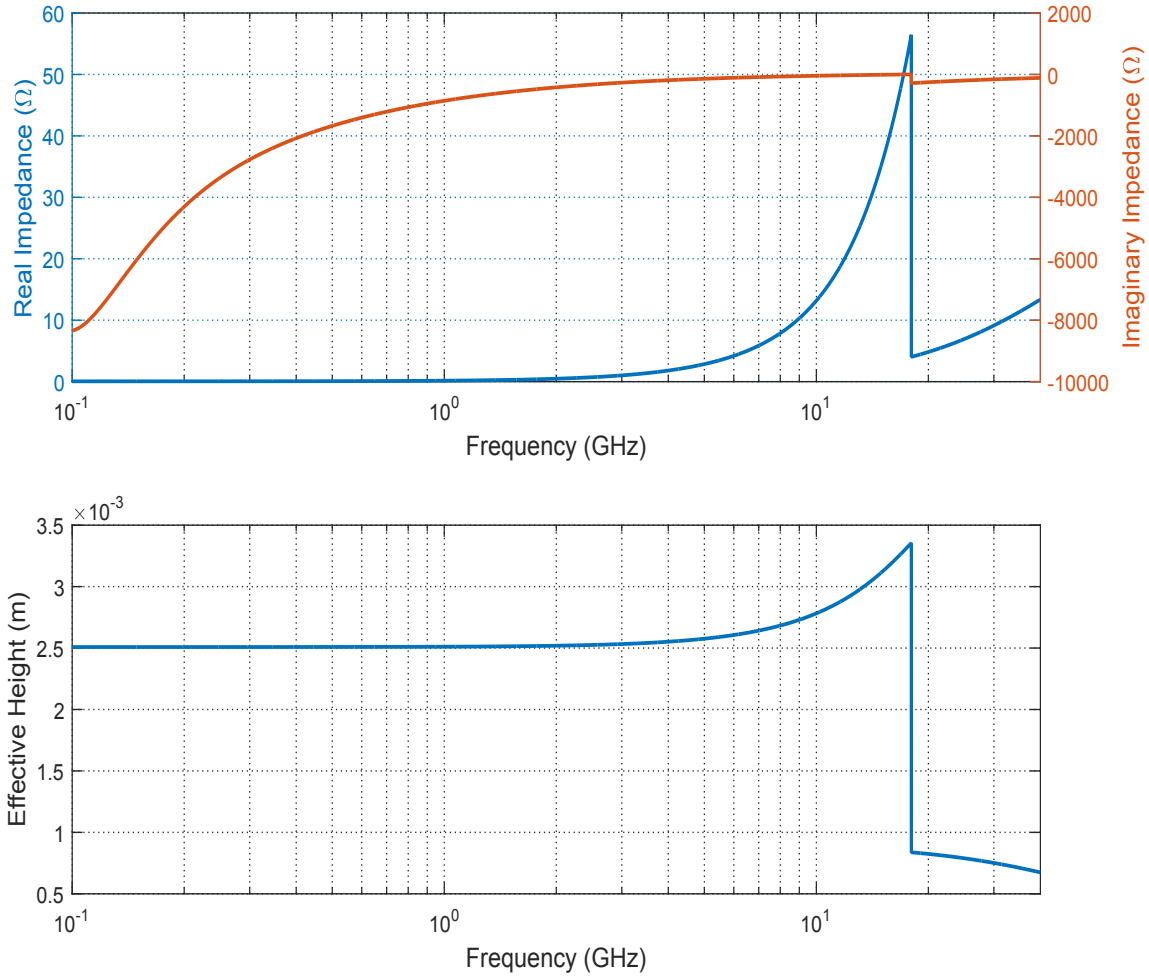

Figure 4: Monopole modeled parameters for E-field conversion data

Equation 7 shows each component of the total E-field in the chamber. The mean value computed here is the mean of the maximum values for each probe location. The overall result, E_{all}, is the average of all eight locations and the three axes.

$$\langle \vec{E}_x \rangle = \frac{\left(\sum \vec{E}_x\right)}{8},\ \langle \vec{E}_y \rangle = \frac{\left(\sum \vec{E}_y\right)}{8},\ \langle \vec{E}_z \rangle = \frac{\left(\sum \vec{E}_z\right)}{8},\ \langle \vec{E}_{all} \rangle = \frac{\left(\sum \vec{E}_{x,y,z}\right)}{24}$$

Equation 7. Three orthogonal E-field components and the aggregate

Equation 8 and

Equation 9 use the results from

Equation 7 to compute the normalized standard deviation of each data set.

$$\sigma = \sqrt{\frac{\sum\left(\vec{E}_i - \langle\vec{E}\rangle\right)^2}{n-1}}$$

Equation 8. Standard deviation of maximum values at eight points

$$\sigma(dB) = 20\log_{10}\left(\frac{\sigma + \langle\vec{E}\rangle}{\langle\vec{E}\rangle}\right)$$

Equation 9. Standard deviation of maximum values at eight points expressed in dB

The IEC standard deviation specification is ≤ 3 dB. The standard allows an increase of standard deviation between 100 MHz and 400 MHz. The limit for standard deviation drops from 4 dB to 3 dB linearly between 100 MHz and 400 MHz. The standard also allows a maximum of three frequencies per octave to exceed the limit by no more than 1 dB[2].

[2] Table B.2 'Field uniformity tolerance requirements' of IEC 61000-4-21

7. RESULTS

Figure 5 shows all the plots of data collected from a single probe during a single test. Each point of each trace represents the result from 1000 measurements during one revolution of the tuner. The instrument controller selects a test frequency and collects data for one revolution of the tuner. This graphic shows two groups of traces. The top traces are the maximum values from each probe axis. The bottom traces are the mean values from each probe axis. It is interesting, although expected, that the variance of the means is significantly smaller than the maximums. The trace 'All' is the combined data set of the three probe axes.

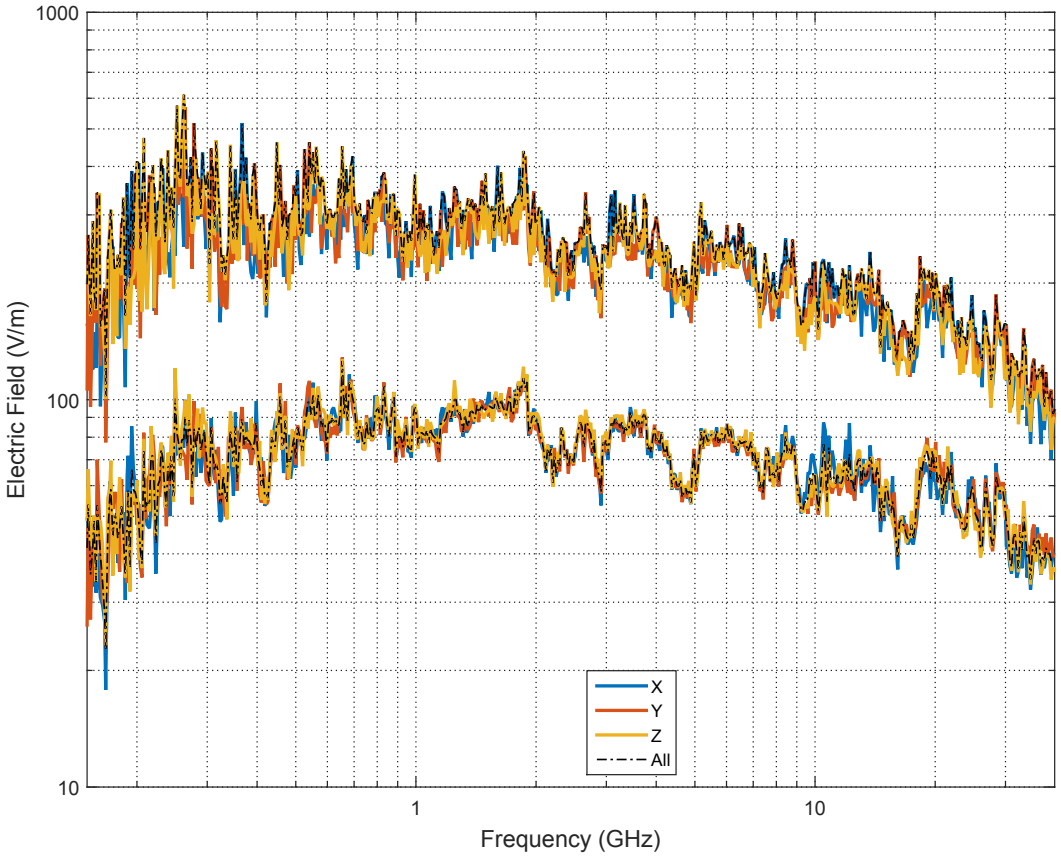

Figure 5: Max and Mean Electric Field Measured Using Electric Field Probes

Figure 6 shows two plots that give an indication of the performance of the chamber. The top figure shows the chi distribution at about 2 GHz. Hence, these data are the 1000 points that produce one point in Figure 5. The three axes and the overall results are a good fit to the theoretical value. The bottom figure shows a goodness-of-fit value for each frequency point. As will be illustrated in other results, the chamber exhibits a good fit to the expected distribution between about 700 MHz and 18 GHz. The chamber performance at low frequency is a consequence of chamber size that causes a reduced number of modes. The reduced performance

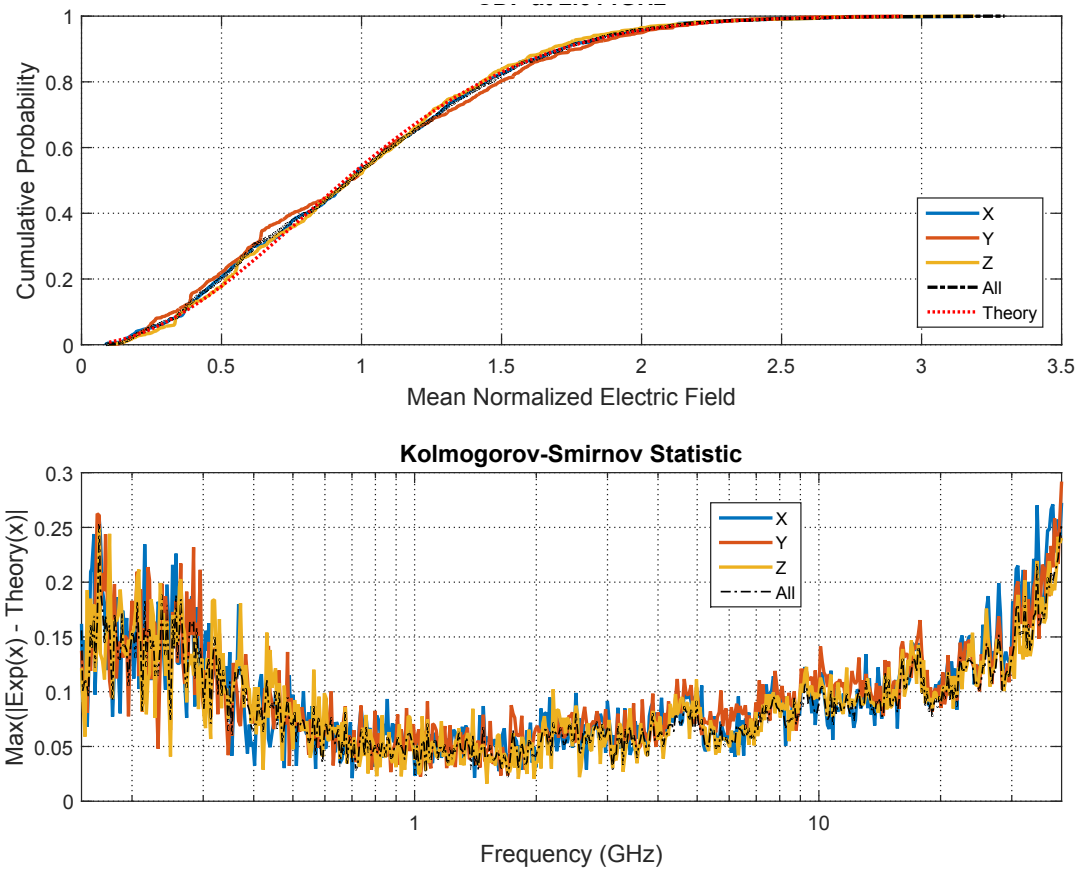

Figure 6: Comparison of Electric Field Measurements with Theoretical Distribution

at high frequency is not a consequence of the chamber but due to ETS probe response time. The rotation speed of the tuner for the test was 30 seconds. Figure 7 show the mean normalized standard deviation with the tuner operating at 30 seconds, 60 seconds, and 120 seconds. As stir time increases, the quality of fit improves above 6 GHz. Further increase in stir time would further reduce the difference between the theoretical value and the measured value.

At higher frequencies, the number of modes and the chamber's sensitivity to changes in tuner position produce rapid changes in field intensity. The ETS probes are not able to make accurate measurements under these conditions. Hence, the phenomena noted in Figure 6 and Figure 7 is a consequence of equipment performance (ETS probes) as opposed to chamber statistics. The monopole antennas mounted on the chamber walls deliver their power to meters. Hence, during normal chamber operation rotation speed is not an issue because the power meters have sufficient bandwidth to make accurate measurements.

It is interesting to note that tuner rate of rotation maybe a factor to test object response. Like the ETS probes, a test object may be sensitive to change in E-field. This does not affect chamber uniformity, but does affect test setup consideration for a specific test object.

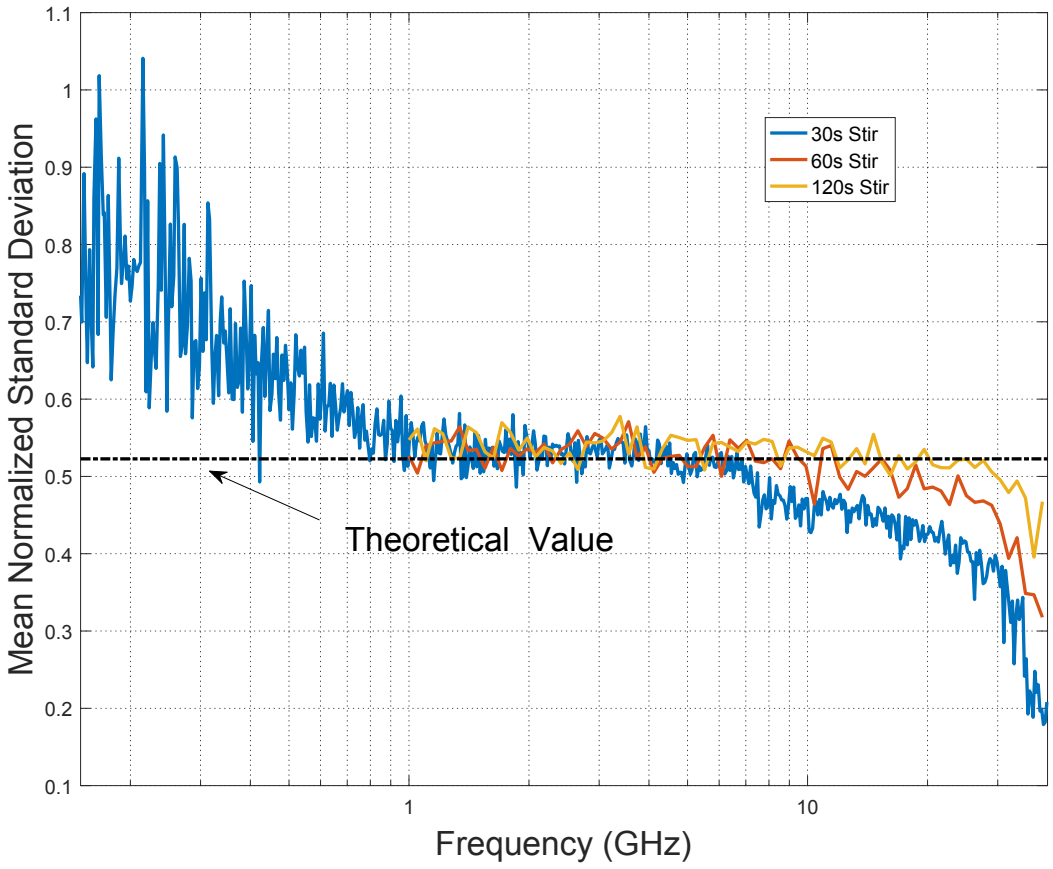

Figure 7: Mean Normal Standard Deviation for different rotation speeds Longer stir periods improvement measured performance. The improvement is a consequence of the ETS probes.

Another metric of chamber performance is the number of identical and independent samples. Using the autocorrelation defined in section 6, Figure 8 shows the estimated number of identical and independent samples. The minimum number of independent samples shown in Figure 8 is 24. At these low frequencies, the number of independent samples still meets the IEC 61000-4-21 requirement of 12 independent samples.

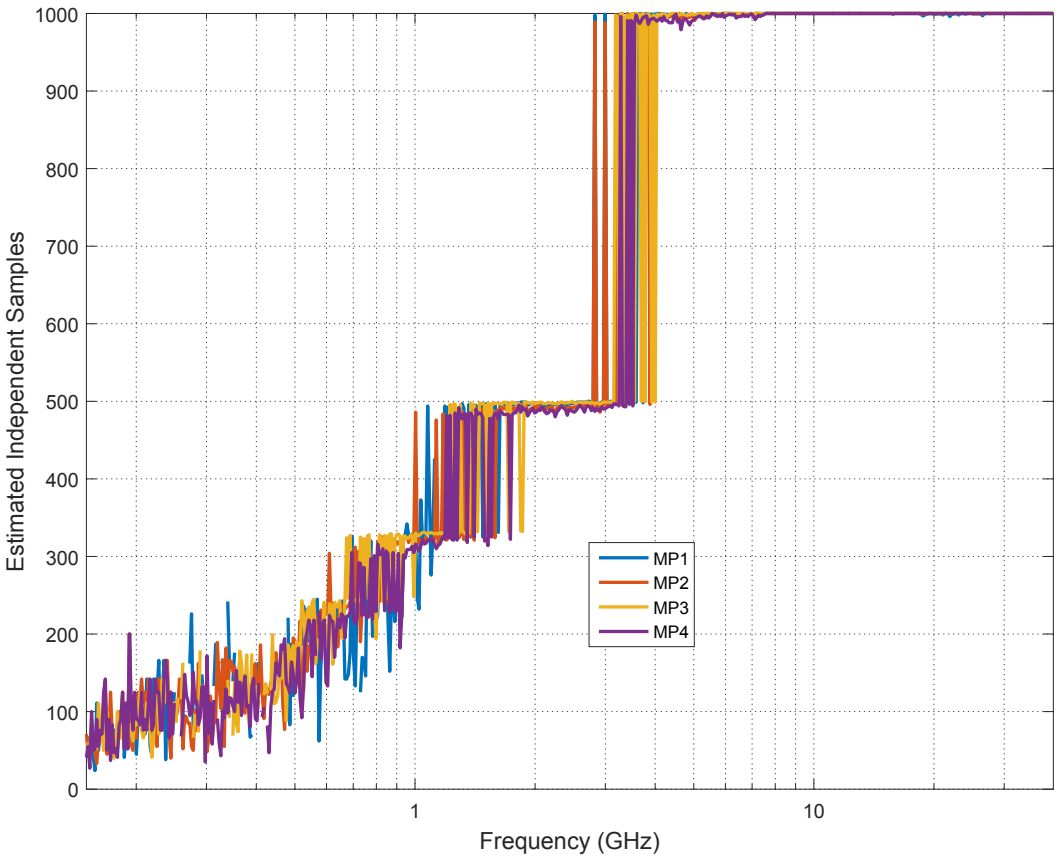

Figure 8: Estimated number of identical and independent samples

Figure 9 shows the power measured by the monopoles mounted on the walls of the reverberation chamber. The top group of traces contains the peak values of each of the monopoles. Each point of each line is a result extracted from a 1000 point measurement over one revolution of the tuner. The bottom group of traces shows the mean values of the four probes. Note that the mean power is just above -50 dBm and never exceeds +10 dBm.

Comparing Figure 9 to Figure 5, the shapes of the curves are very different. The difference is a consequence of the performance of the monopoles (Figure 4). Once the monopole corrects are employed Figure 9 turns into Figure 5

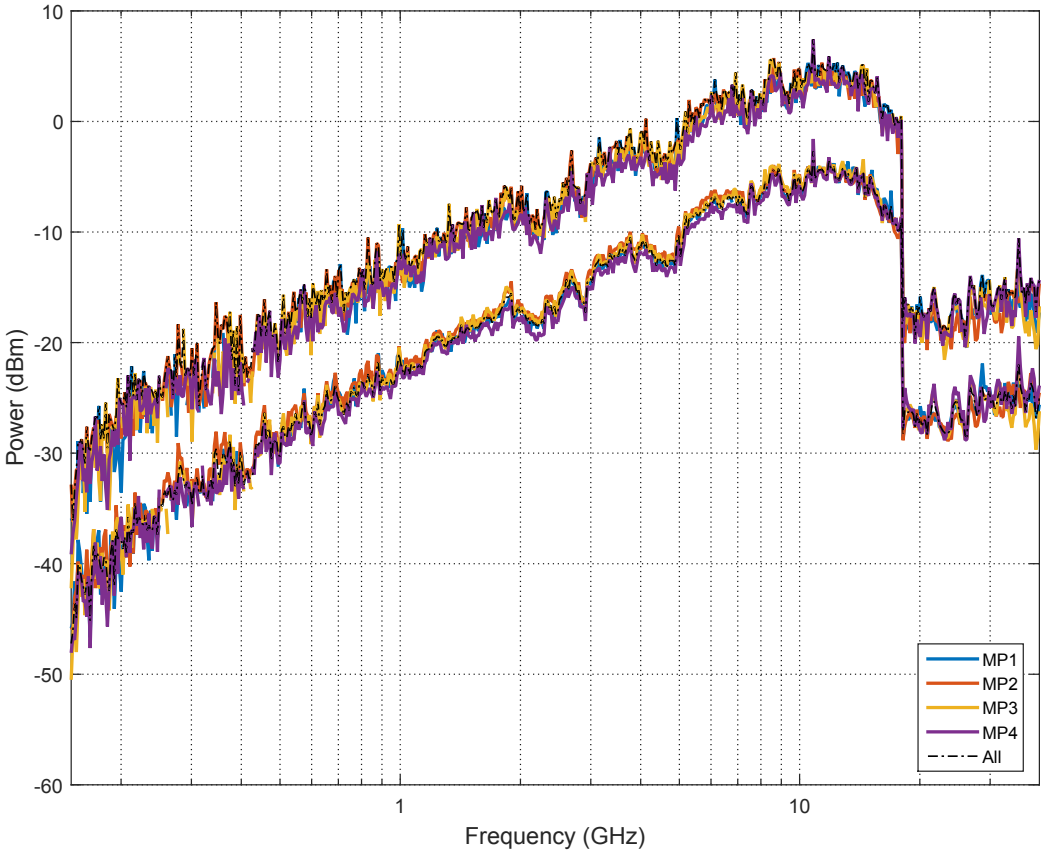

Figure 9: Max and Mean Received Power from Monopole Sensors on Walls

Figure 10 shows the electric field computed from the power readings shown in Figure 9. The power meter readings increased 20 dB per decade (see Figure 9) as expected for a monopole. Using the correction factors for both the 4.3 mm and 0.0 mm probes, the electric field is accurately presented in Figure 10.

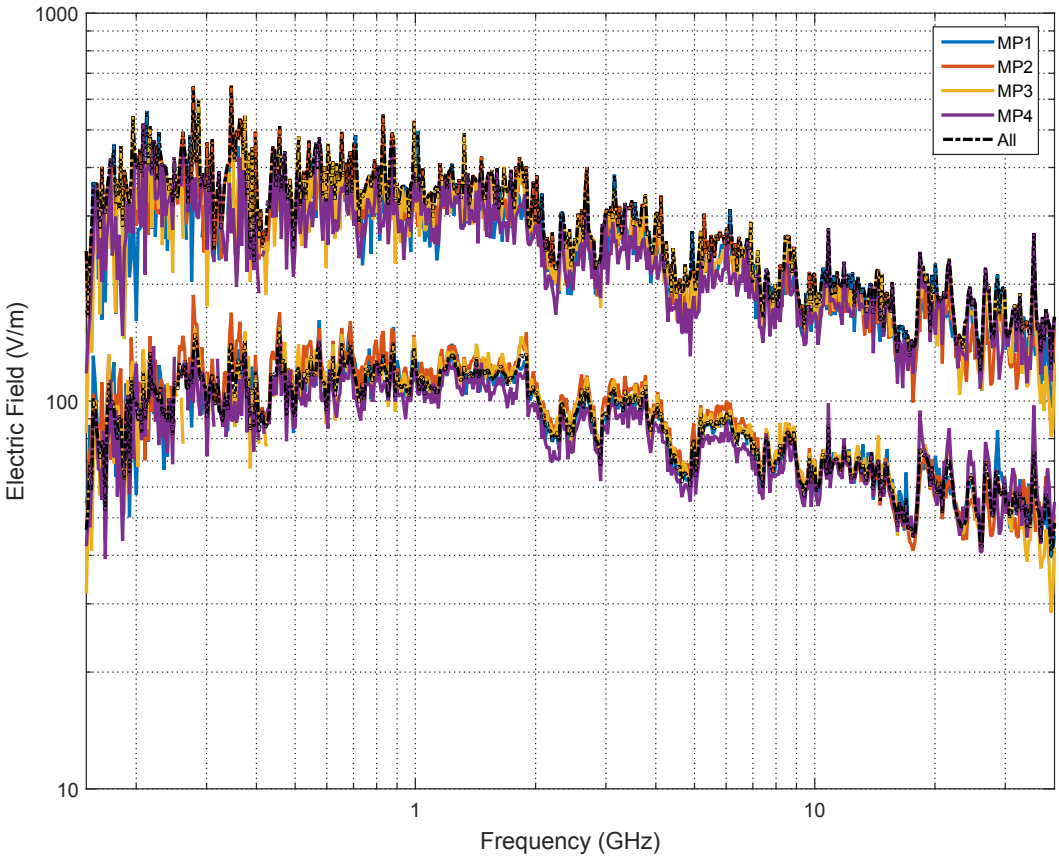

Figure 10: Electric Field Calculated from Monopole Measurements

Figure 11 illustrates the statistics of the data collected by the monopoles. The cumulative distribution function, for all four monopoles, agrees with the expected values. Recall the response of the ETS probes showed a deviation from theory at higher frequencies. Comparison of the monopole results and the ETS probe results (Figure 6) is further evidence that the deviation seen by the ETS probes are due to the time response of the ETS probes not chamber behavior.

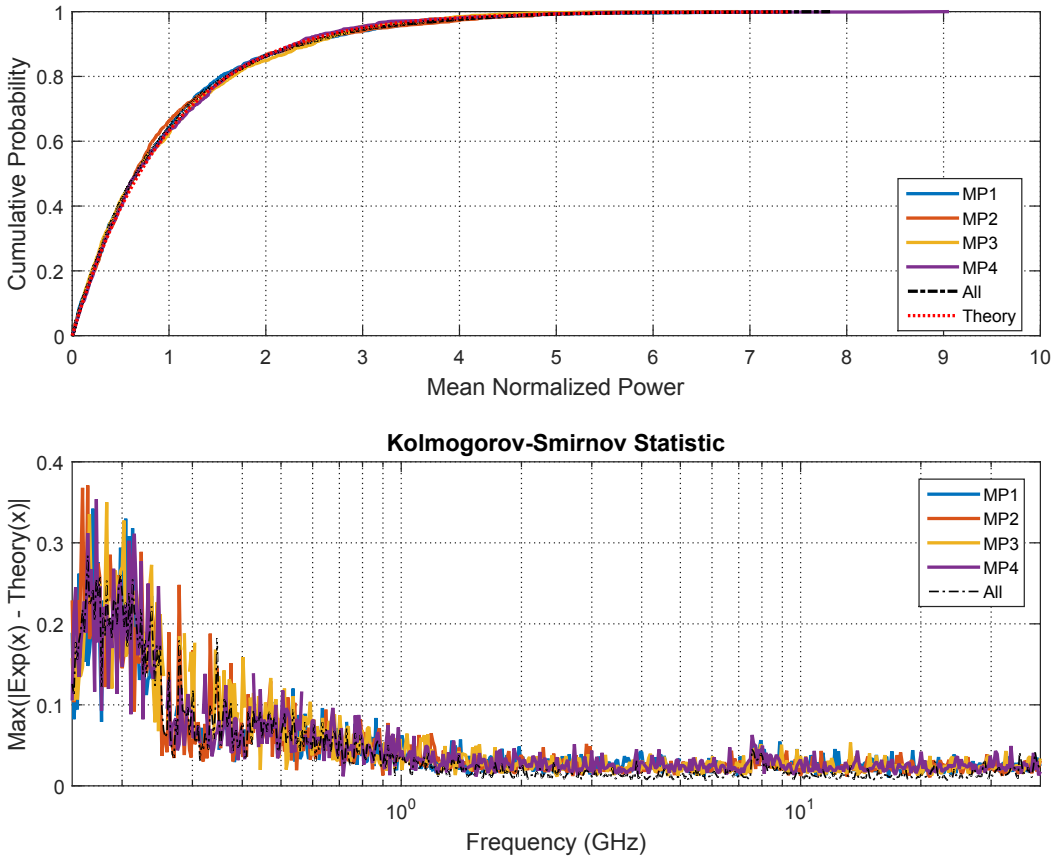

Figure 11: Cumulative Distribution Function for Power Readings

Figure 12 shows the computed standard deviation for the large volume, consisting of the eight corners using the top and bottom probes on the probe stand. The dotted "Limit" line in the plot is a reference to the limit per IEC 61000-4-21. Each location contained three probes with 3 axes elements. The results meet the requirements of the standard. The standard allows the limited number of excursions that exceed the limit at low frequency.

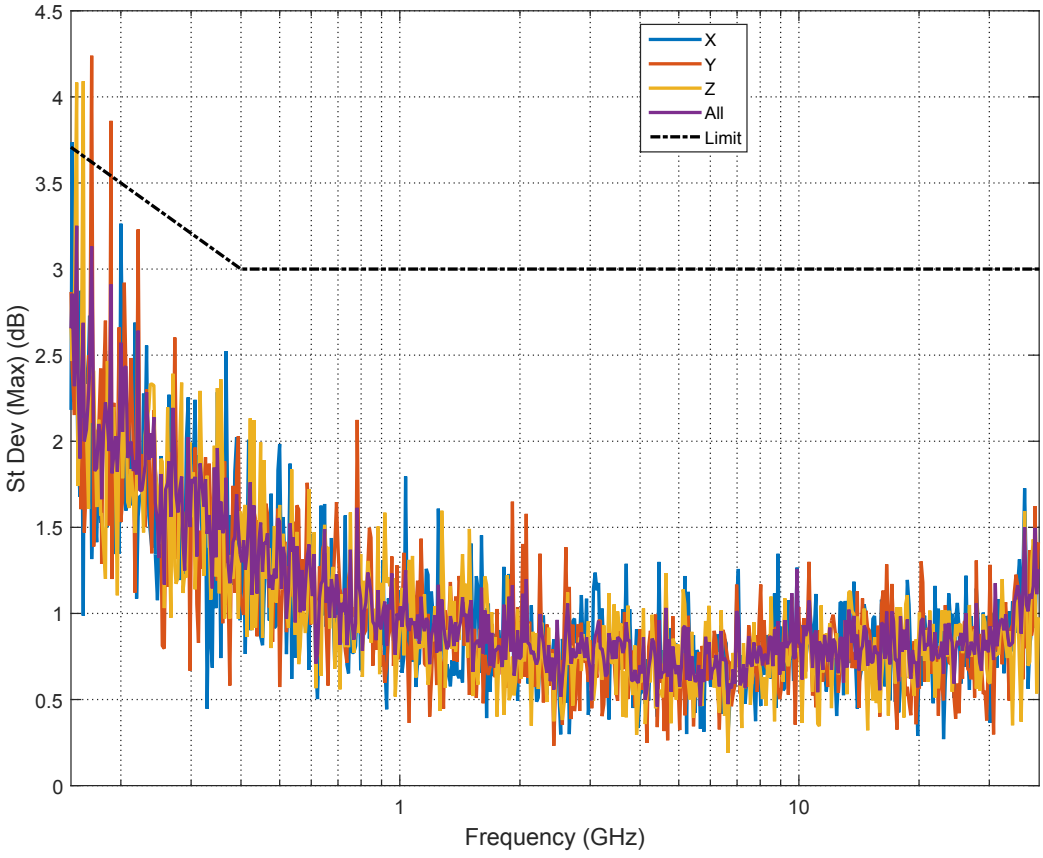

Figure 12: Standard Deviation of 8 Corner Points of Working Volume

As mentioned earlier in this report, initial measurements revealed that the ETS probes have a limited time response. The consequence is evident in Figure 7. While obtaining the longer time measurements, we also looked at smaller volumes within the reverberation chamber. Figure 3 shows the volumes for the next set of results. The top volume (Volume 1 in Figure 3) and the bottom volume (Volume 2 in Figure 3) combined to create a total volume. The following results come from 120-second tuner revolutions. The frequency range and sampling density is less for this limited excursion than the full data set collected in 2015. The purpose of these results is to illustrate the difference in chamber performance for a smaller volume and longer tuner rotation time. Figure 13, Figure 14, and Figure 15 show good agreement for E-field in all directions. They also show the standard deviation is about 1 for all frequencies.

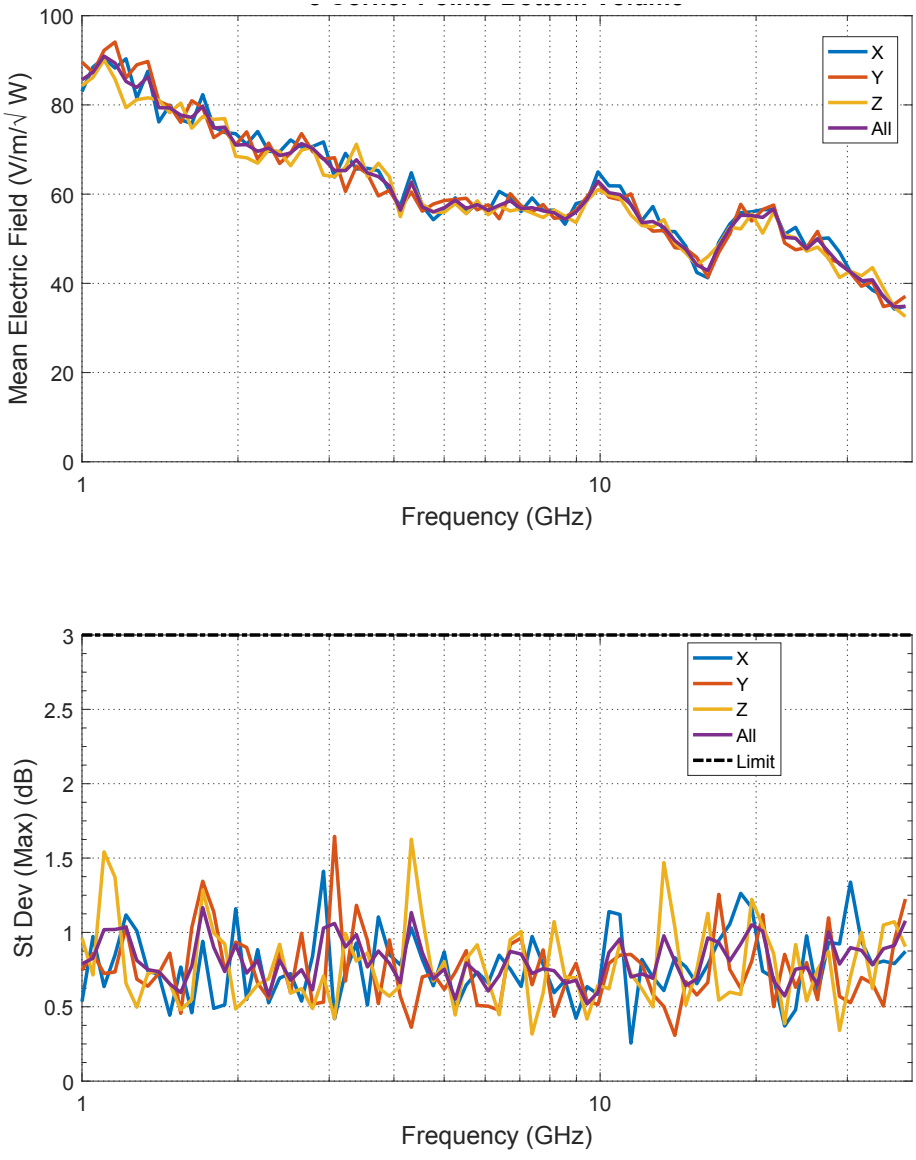

Figure 13: Lower Volume

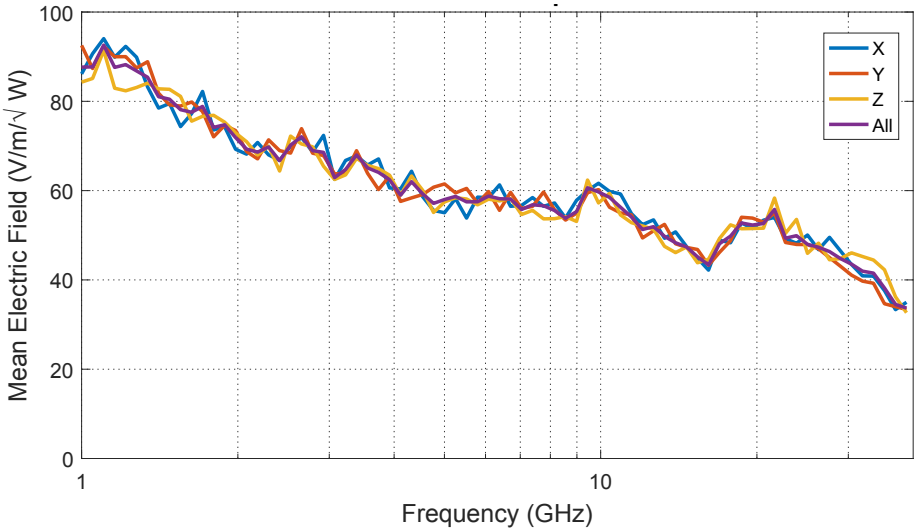

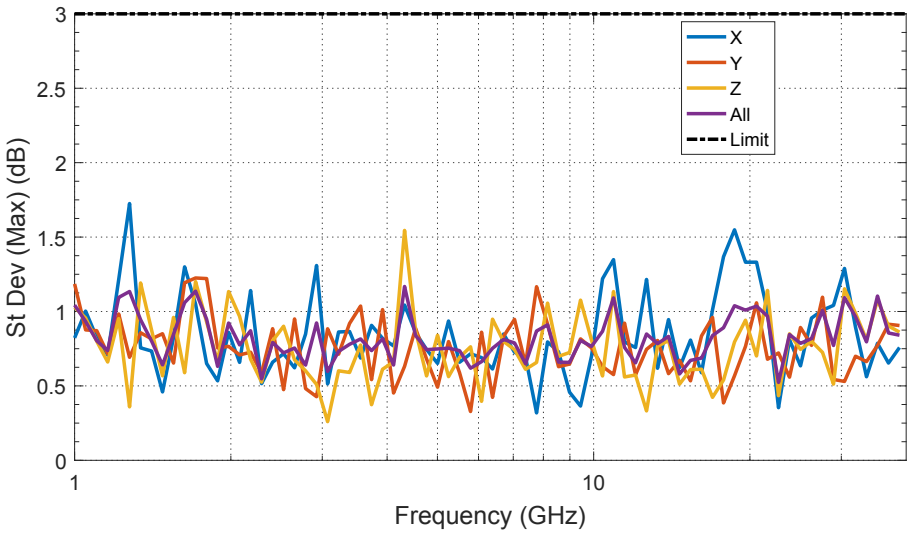

Figure 14: Upper Volume

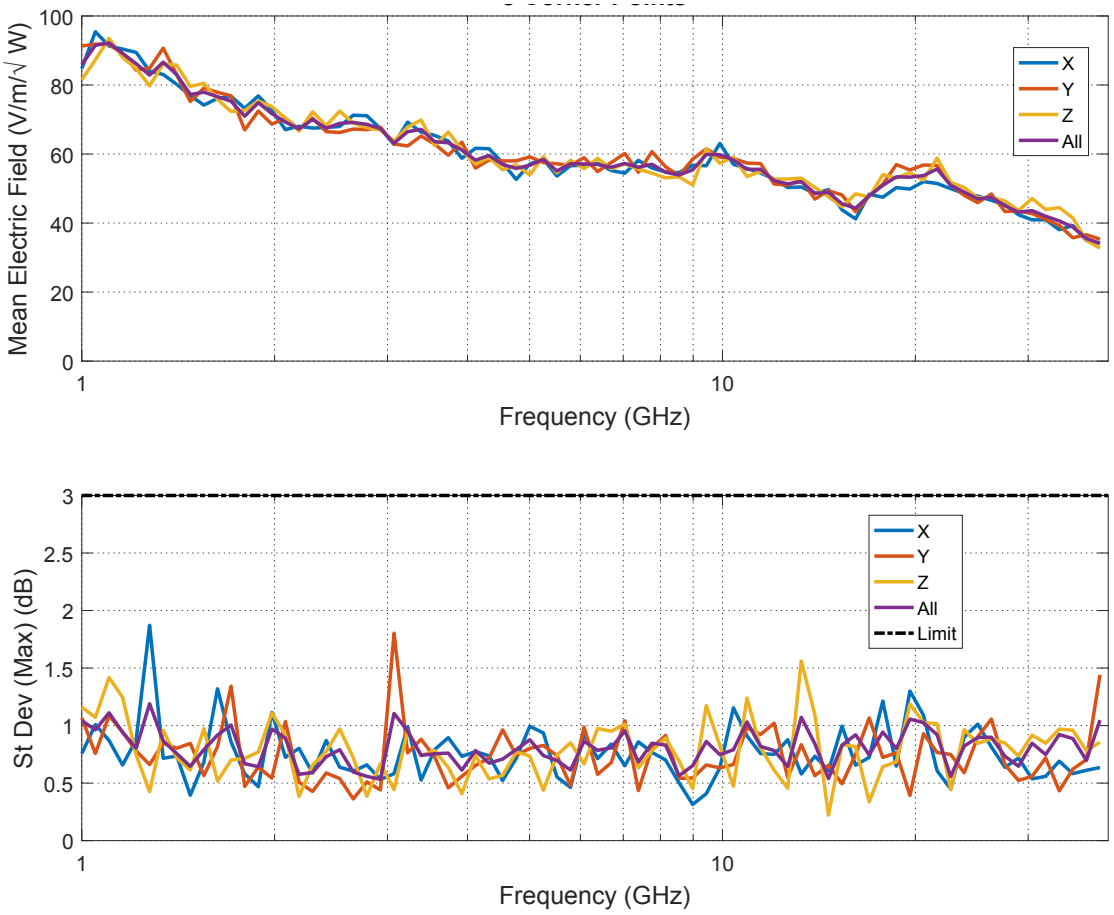

Figure 15: Total volume

Figure 16 shows the mean normalized standard deviation for the reduced data collection total volume. Note that the value drops above 20 GHz. This drop is a consequence of the ETS probe limited response time. All the elements of the ETS probe agree about the normalized standard deviation of the E-field. As stated earlier, this deviation from the ideal response is a consequence of the ETS probes not the chamber.

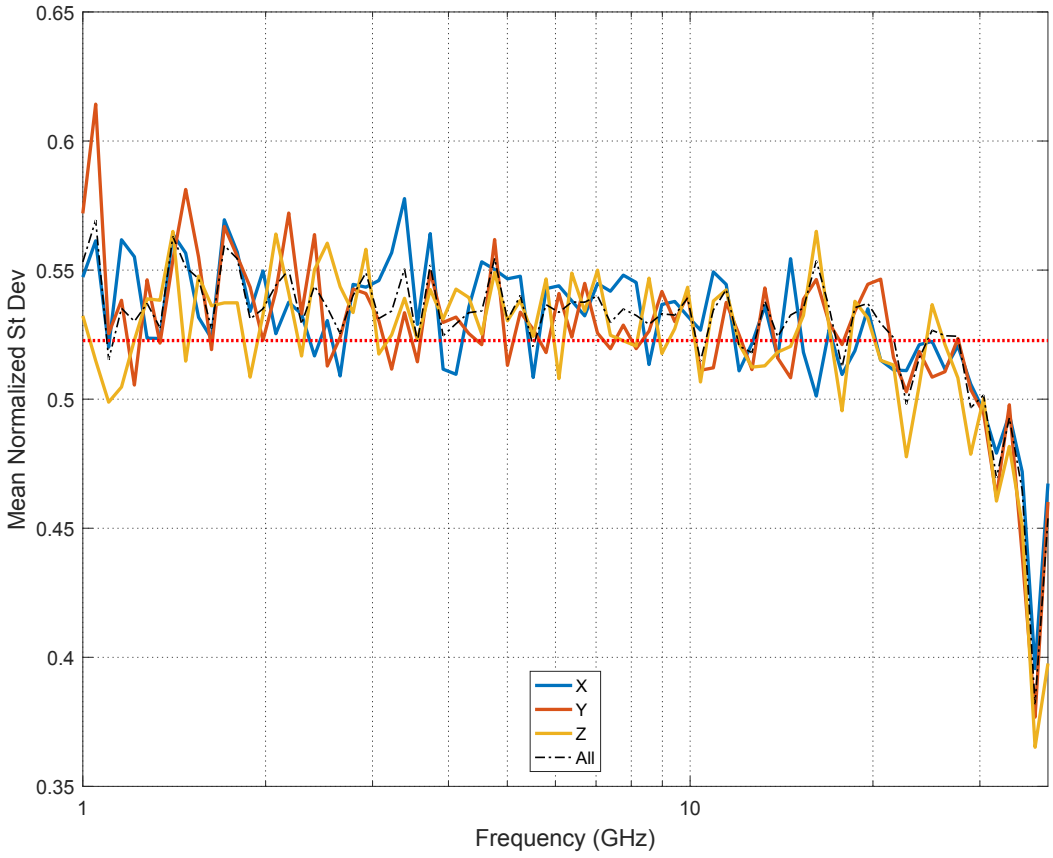

Figure 16: Reduced data collection

Figure 17 shows computed E-field maximum values from ETS probes and the 4 monopoles. The figure shows averages of the maximum reading from either 1000-monopole readings or the 1000 ETS probe readings at each frequency. This figure also shows the difference between the field measurements and the monopole readings. The ETS probes consistently reported lower field strength than the monopoles. The difference is as high as 5 dB. Recall the monopoles mount on the chamber walls. Earlier in this report was a discussion regarding the response time of the ETS probes.

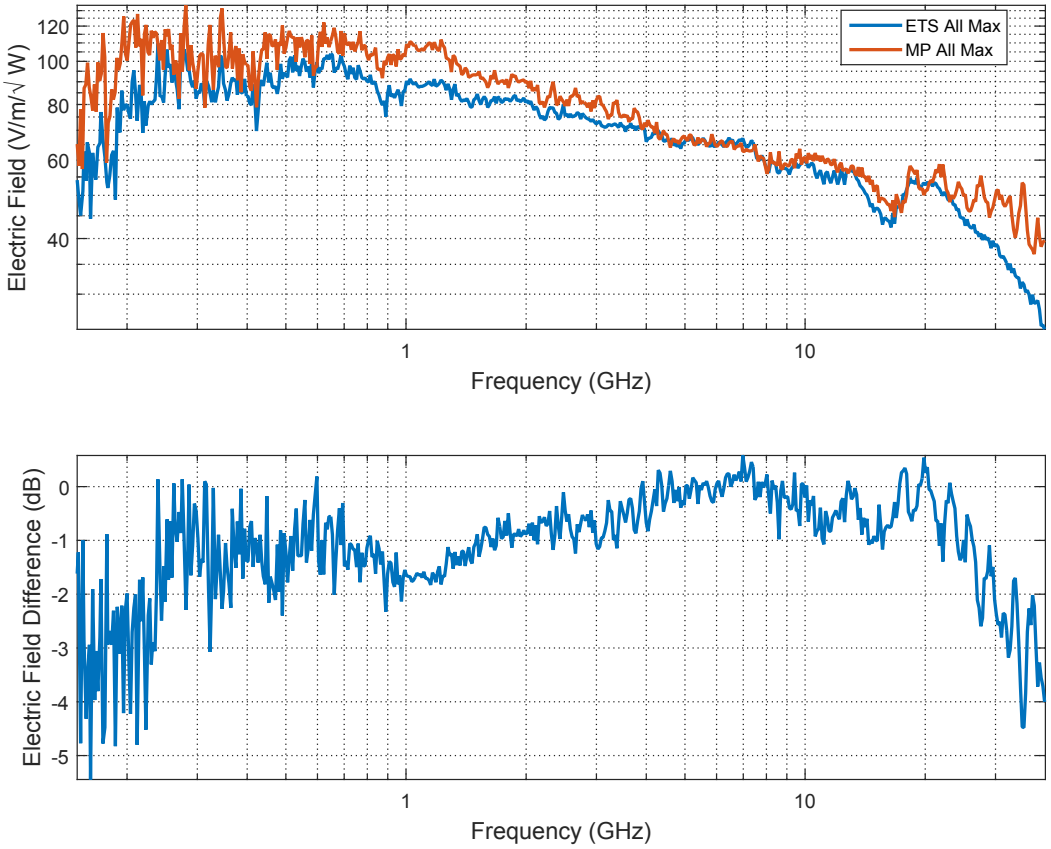

Figure 17: Comparison of Monopole and Electric Field Probe Measurements

Figure 18 shows the same results as Figure 17 with 120-second tuner rotation time. Again the results show as much as 1 dB difference at 1 GHz. Recall the earlier result showed as much as 1.5 dB difference around 1 GHz. The first results compare the maximum readings; the later results compare the mean values. According to the IEC61000-4-21 standard, any variation greater than 3dB between probe and antenna measurements should be resolved, although agreement is not expected at the lowest frequencies due to the statistical nature of the reverberation chamber. Longer stir times resolve the discrepancy at higher frequencies seen above, while the total variation is still low.

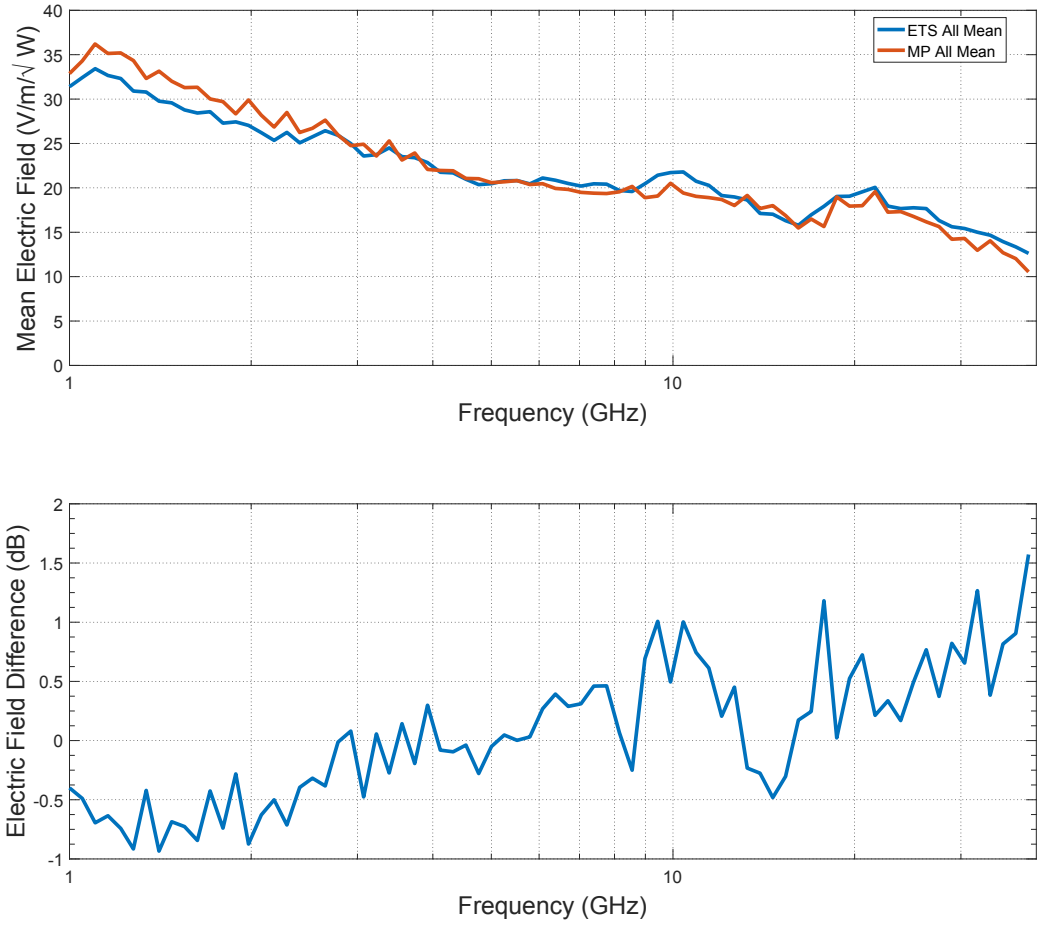

Figure 18 Comparison of ETS probe and monopoles E-field strength

Recommended Application of This Data

Test results of the reverberation chamber shows that the chamber meets the requirements of IEC 61000-4-21. Any tests conducted in the chamber can use the standard as a reference for E-field uniformity and thereby uncertainty. It should be noted that test objects placed in this facility will have an effect on the field structure. The size of the object and materials that it is created from will determine the significance of that impact.

Results comparing the electric field measured in the center of the chamber compared to the predicted electric field measured by the monopoles on the wall show good agreement above roughly 250MHz, within about 2dB. At lower frequencies, greater variation is expected due to the undermoded statistics of the chamber. Although not unexpected for different measurement types, this variation can be included in the overall uncertainty associated with the exposed field in the chamber as measured by the monopoles located on the wall.

8. REFERENCES

1. "Reverberation chamber test method," *IEC Standard 61000-4-21, Electromagnetic Compatibility (EMC), Part 4-21: Testing and Measurement Techniques – Reverberation chamber test methods*, Edition 2, 2011.
2. Forbes, Catherine, Evans Merran, Hastings Nicholas, Peacock Brian, (2011) *Statistical Distributions,* John Wiley and Sons, pp. 69-73.
3. Course Notes from *Reverberation Chamber Theory/Experiment Course, Sep2011, Oklahoma State University, REFTAS*
4. Chakravarti, Laha, and Roy, (1967). *Handbook of Methods of Applied Statistics, Volume I*, John Wiley and Sons, pp. 392-394.
5. Forbes, Catherine, Evans Merran, Hastings Nicholas, Peacock Brian, (2011) *Statistical Distributions,* John Wiley and Sons, pp. 74-76.

DISTRIBUTION

1	MS0899	Technical Library	9536 (electronic copy)
10	MS1152	Robert Salazar	Org. 1353
1	MS1152	Robert Salazar	Org. 1353 (electronic copy)
1	MS1152	Steven Glover	Org. 1353 (electronic copy)


Sandia National Laboratories